THE RESPONSE OF A 4π NEUTRON DETECTOR BUILT FOR K-500 SUPERCONDUCTING
CYCLOTRON AT TEXAS A&M UNIVERSITY

A Thesis
by

ISAAC HONGBIN LIU

University Undergraduate Fellow, 1989–1990
Cyclotron Institute, and Department of Chemistry
Texas A&M University

Submitted to University Honors Program of
Texas A&M University
in partial fulfillment of the requirements for the degree of

BACHELOR OF SCIENCE

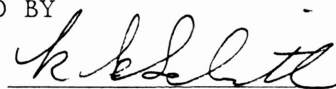April, 1990

Major Subject: Chemistry

THE RESPONCE OF A 4π NEUTRON DETECTOR BUILT FOR K-500 SUPERCONDUCTING CYCLOTRON AT TEXAS A&M UNIVERSITY

Isaac Hongbin Liu

University Undergraduate Fellow: 1989–1990
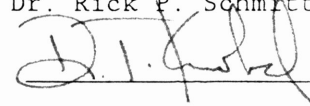Cyclotron Institute, and Department of Chemistry
Texas A&M University

APPROVED BY

Fellows Advisior: _____

Dr. Rick P. Schmitt

Honors Director: _____

Dr. Dale T. Knobel

ACKNOWLEDGMENTS

I wish to express my sincere gratitude to my research advisor, Dr. Rick P. Schmitt for his guidance and patience throught my undergraduate research projects. I would to thank him for the tremendous confidence he has kept in my work for the past two and half years. As an instructor, advisor, and leader, he has provided the major impetus for the production of this work.

I also wish to thank Honors Director, Dr. Dale T. Knobel, and Julie Conley in the Honors Program, whose long hours and hard work kept this Fellows program going.

The work of other group members, B. Hurst, L. Cooke is appreciated.

Finally, my family has always stood beside my efforts. Knowing that my father, Dr. Jiarui Liu, my mother, Dr. Guiju Yu, and my brother, Hongbiao, were interested in my work and confident in my abilities has always been a source of inspiration. Their enthusiasm for my work surpassed my own at critical times, and so has provided immeasurable motivation and encouragement. I look forward to a lifetime of sharing their good spirit, their optimism, and their love.

Table of Contents

The Responce of A 4π Neutron Detector Built for K-500 Superconducting
Cyclotron at Texas A&M University

Isaac Hongbin Liu

Fellow Advisior: Dr. Rick P. Schmitt

Cyclotron Institute, and Department of Chemistry, Texas A&M University, College
Station, Texas 77843

ABSTRACT

A 4π neutron detector which has a relatively high efficiency for detecting
neutrons emitted in nuclear reactions has been constructed. This new 4π neutron
detector has been designed to be much more flexible than the traditional fission
tank used in off line measurements. The most important quantity to be determined
for this detector is the response function, i.e., the efficiency as a function
of the neutron energy. Monte Carlo methods are used to simulate the response of
the detector. Comparisons between the theoretical and the measured efficiencies
should provide the basic information about the characteristics of the detector
which is to be used for in-beam studies with the new K-500 superconducting
cyclotron at Texas A&M University. Further modifications and applications of the
Monte Carlo simulation program are also discussed in this thesis.

INTRODUCTION

The intermediate energy heavy ion beams produced by the new superconducting K-500 cyclotron at Texas A&M University offer new opportunities to investigate nuclear dynamics and the properties of highly excited nuclei. Studies of reaction mechanisms in this energy region present challenging experimental problems.

Frequently, these nuclear reactions produce excited fragments which, in turn, decay by emitting neutrons and light charged particles, for example, the nuclei of hydrogen and helium atoms. These complex secondary decay processes of the reaction products and possible contributions from multiparticle exit channels make it impossible to completely characterize the system which is originally produced in the nuclear collision with simple detection systems. High geometry detectors are clearly needed to carry out experiments in this energy domain. To meet this need, our group, Dr. R. P. Schmitt's group, and Dr. J. B. Natowitz's group have constructed a detector which has a relatively high efficiency for detecting the neutron emitted in the nuclear reactions. This 4π neutron detector is designed to measure neutron multiplicities in heavy ion collisions. Since the number of neutrons (the neutron multiplicity) produced provides a measure of the energy released in a collision, this device, which we called the neutron ball, is basically a calorimeter (see fig. 2).

THE CHARACTERISTICS OF THE 4π NEUTRON DETECTOR

A. Operating Principles

The operating principles of the neutron ball are far from new. In fact, detectors of this type were first constructed in the 1950's. Monte Carlo computer codes have also been developed for modeling these devices. However, these previously constructed systems were built for off-line studies and exhibit rather simple geometries. The neutron ball is a more complex device with a significantly different geometry.

Let us briefly consider the operating principles of the neutron ball. This device is an approximately spherical tank filled with nearly two thousands liters of hydrocarbon based, liquid scintillator. The scintillator tank becomes very efficient neutron detectors when it is loaded with one third of a percent gadolinium by weight. Gadolinium has two isotopes, ^{155}Gd and ^{157}Gd with 15 and 16% abundance respectively, which have very high thermal neutron capture cross sections of $6.1 * 10^4$ and $2.5 * 10^5$ barn. The probability that a neutron is captured in the time interval (t, t+dt) measured with respect to the nuclear reaction is expected to follow the empirical formula

$$h(t) \propto e^{-\alpha t}[t(\beta-\alpha)-1]+e^{-\beta t}$$

Where α depends on the moderating properties of the scintillator and β is proportional to the Gd concentration.

When a nuclear reaction occurs inside the detectors, energetic neutrons pass through the walls of the reaction chamber and enter into the tank (see fig.1). The kinetic energy of the neutrons is rapidly dissipated mainly via collisions with protons in the scintillator. While some neutrons may eventually escape the detectors, the majority of them become thermalized in the scintillator. When a

6

thermal neutron encounters a gadolinium nucleus, it is absorbed with a high probability. After a neutron is absorbed, several gamma rays are emitted. The latter also interact with dopants in the scintillator eventuallyt producing flashes of visible light. The light flashes are detected by an array of twenty photomultipliers which view the tank through glass windows. Thus by counting the number of these delayed flashes, we can determine the number of neutrons produced in the nuclear reaction.

The neutron multiplicity is then obtained by counting the number of delayed flashes during a counting gate, typically thirty five to eighty microseconds wide. Neglecting the energy dependence of the efficiency and complications due to the background, pile up, etc., the response of a tank to a cascade of neutrons follows the binomial distribution:

$$P(n,k) = \binom{n}{k} * e^k * (1 - e)^{n-k}$$

n represents the true multiplicity;
P(n,k) represents the probability of observing k of the n neutrons;
k represents the number of detected neutrons;
e represents the total efficiency.

With good resolution, the neutron ball will measure not only the mean multiplicity of the neutrons, but the higher moments of the multiplicity distribution as well. Information on these higher moments of the distribution could provide new insights into the energy dissipation mechanisms in heavy-ion collisions.

B. Structure and Characteristics of the 4π Neutron Detector

The neutron ball has a much more complex geometry and is more flexible than the previously constructed scintillation fission tanks. There are mainly three parts in the neutron ball: upper hemisphere, medium plane, and lower

hemisphere (see fig.2). This 4π neutron detector is 156cm in diameter, and contains approximately 2000 liters of liquid scintillator. A 40cm diameter cylindrical reaction chamber is located in the center of the medium plane, which provides adequate space for PPAC's, telescope arrays, and other small trigger detectors. The chamber has a wedge-shaped extension in the forward direction since many reaction products, for example, the evaporation residues and fragmentation products, are strongly focused in the forward direction. The division of the tank allows access to the reaction chamber. The medium plane is divided into ten modules which can be removed to mount external counters, such as gamma ray counters, large ionization chambers, without greatly compromising the efficiency of the neutron ball (see fig.3).

The size of the neutron ball is shown on fig.4.

The neutron ball and the reaction chamber are built from aluminum to minimize activation. The internal walls are relatively thin to minimize absorption, and the outer shell of the tank is relatively thicker to limit the deformation of the ball and to provide for the mounting of the phototubes and the support structure. This neutron detector is supported on the bottom by adjustable legs which can provide some movement. The upper and lower hemispheres can be used even without the central ring modules.

There are total twenty photomultipliers mounted on the neutron ball: five on the upper hemisphere, ten on the medium plane, and five on the lower hemisphere. The phototubes view the liquid scintillator tank through glass lenses. Steel compression rings push the glass lenses against O-rings to seal the hemisphere. All phototubes are encased in soft iron canisters to provide some magnetic shielding for the phototubes. Dry nitrogen gas is circulated through the canisters to prevent the possibility of explosion due to sparking.

MONTE CARLO SIMULATION OF THE 4π NEUTRON DETECTOR

Like any other instrument, the neutron ball must be calibrated to allow raw experimental data to be converted into physically significant quantities. The most important quantity to be determined is the response function, i.e., the efficiency as a function of the neutron energy. The comparisons between the theoretical and the measured efficiencies should provide the basic information about the characteristics of the detectors needed for in-beam studies with the K-500 superconducting cyclotron.

A. Monte Carlo Method

Monte Carlo method, which is technique for estimating the solution x or y of a numerical mathematical problem by means of an artificial sampling experiment, is used to simulate the detection process to determine this 4π neutron detector's efficiency. The importance of this method arises primarily from two important sources: the practical need to solve equations that are too long and complicated to solve by using analytical methods alone, and the increased importance of all numerical methods because of the advent of the high speed computer systems. The main justification for the name Monte Carlo is that during the 1950's several tricks were introduced for improving the efficiency of this method, so that the subject has assumed a new flavor.

One of the earliest examples of the use of Monte Carlo method was introduced by the French naturalist G. L. L. Buffon in 1773 to estimate the value of π. The method he used is to throw a needle on a striped handkerchief and see how often it falls touching more than one stripe. If the width of each stripe is equal to the length of the needle, then the proportion of successes will be close to $2/\pi$ for a long series of trials.

The main advantage of the Monte Carlo methods is that they do not become much more complicated when the physical dimensionality of a problem is increased, and therefore provides opportunities of obtaining qualitative information about solution of partial differential equations in three or more dimensions and about the values of multidimensional definite integral. This method has been applied to a wide range of areas, include autoregressive time series, size of cosmic ray showers, critical size of nuclear reactors, other neutron transport problems, and Schrodinger's partial differential equation.

B. Calculation Process of the Method

The Monte Carlo simulation program which is applied in the neutron detector was first introduced by two French scientist: J. Poitou, and C. Signarbieux in 1974. The Monte-Carlo calculation process, which is defined by Reines, Cowan, Harrison, and Carter, "assumed that all relevant parameters materially affecting the slowing down and capture of neutrons in an isotropic homogeneous mixture of hydrogen and cadmium (gadolinium is used in our detector) atoms could be properly represented in terms of relative probability." For each neutron there exist three quantities associated with its detection:

(1)   Slowing down in the liquid scintillator, and being captured by the gadolinium. This yields the capture efficiency ϵ_c;

(2)   Emission of the gamma rays and their interactions with the hydro-carbon based liquid scintillator. This gives rise to the gamma ray detection efficiency ϵ_γ;

(3)   Photon emission and collection by the photomultipliers giving the light-collection efficiency ϵ_l;

Therefore the total efficiency can be written as the following:

$$\epsilon_{total} = \epsilon_c * \epsilon_\gamma * \epsilon_l$$

10

In the Monte-Carlo simulation code, only first two steps were included, which are the capture efficiency and the emission of the gamma ray cascade and their interaction with the liquid scintillator.

The main program first calls the subroutine LOC, which takes care of the initialization and the input of different cross sections. The second step involves that the main program initiates a loop on the events. The subroutine RALENT computes the type of interaction, the interaction range, the final energy of the neutron, and the direction vector of the neutron. After this is finished, RALENT calls the GEOM to calculate the trajectories, the path through the vacuum and then escape. RALENT returns the control to the main program if any one of the following three conditions is satisfied:

(1) The neutron is captured by the gadolinium;

(2) The neutron escaped from the neutron ball;

(3) The limit of counting time gate is reached (usually 36 to 80 microseconds).

If the first condition is satisfied, the main program will call the subroutine SLOWIN to simulate Compton scattering. After all these have finished, the main program will make an statistical analysis, and then calculate the total efficiency for detecting neutrons (the flowchart of this program is shown in fig 5).

CALIBRATION OF THE 4π NEUTRON DETECTOR

A. Modified Monte Carlo Method

Several developments on the Monte Carlo simulation program have been made these two years:

A huge data base file that contains essentially all the information about the neutron ball was first generated by array generator Fortran-77 file. This

data file is basically a three dimensional array which describes the neutron ball geometry. The array contains 100^3 (1 million) grid points. Equations that specify different planes (top and bottom planes of the reaction chamber, wedges, and vacuum pipes, etc.) have also been written in the array generator fortran file.

Grid points in different spaces (such as in the vacuum part or in the liquid scintillator part) have been assigned with different integer numbers: 0 for evacuated parts, include reaction chamber, beam pipe, and two 20° forward chamber wedges; 1 for parts in the liquid scintillator, and 2 for the parts inside the array but outside the neutron ball. By completing this part of the program, the position of the gamma ray and neutron can be easily identified in the Monte Carlo simulation program. Several relatively simple models have been made first, and tested for the calculation of trajectory between two interactions inside the neutron ball. The computer calculated distances are in excellent agreement with the true distances: resulting in only about 2% error.

B. New Geometry Model

The second part of the modification process was to rewrite the GEOMETRY subroutine. The rewritten GEOMETRY subroutine is a relatively long code due to the complexity of this 4π neutron detector's structure.

The main simulation program and other subroutines were changed as little as possible. Since the main program calls the GEOMETRY subroutine so many times, it is going to take extremely long CPU time if the "CALL ARRAY" command was placed inside the GEOMETRY subroutine; therefore, several commands were added to the main program to open the neutron ball array data file. A "COMMON ARRAY" command was added to the main program and all other related subroutines in order to make the array universal transferable.

The new GEOMETRY subroutine first accepts a series of data from the main

program: the neutron ball array data file; the direction of the neutron generated by a random number generator: their cosine value in x, y, and z direction; the initial position of the neutron in x, y, and z coordinates; and the path length travelled by the neutron which is also generated by the random number generator,

A series of transformations on the coordinates was performed, since the GEOMETRY subroutine and the main program have different origins on the Cartesian coordinates.

The GEOMETRY subroutine calculates the number of grid points that the neutron has travelled through the neutron ball array. The distance that travelled in the vacuum part of the detector is added to the total distance travelled by the neutron.

In the final part of this subroutine, the program calculates the final position of neutron, its corrected path length, and returns these values to the main simulation program.

RESULTS

A. Monte Carlo Simulation Results

Data for 1.0, 3.0, 5.0, and 7.0 MeV (see next page)

```
------------------------------------------------------------
  RESULTS FOR   1.00 MeV NEUTRONS    200 ITERATIONS

        0 NEUTRON ESCAPES
        0 WITHOUT INTERACTION WITH THE DETECTOR

        3 NEUTRONS CAPTURED BEFORE        1.00 MICROSECONDS
       13 NEUTRONS NOT CAPTURED WITHIN   80.00 MICROSECONDS
      184 NEUTRONS CAPTURED IN THE COUNTING GATE

    THRESHOLD    GAMMA EFFICIENCY    TOTAL EFFICIENCY
       0.2           0.957               0.880
       0.6           0.940               0.865
       1.0           0.929               0.855
       1.4           0.891               0.820
       1.8           0.864               0.795
       2.2           0.826               0.760
       2.6           0.783               0.720
       3.0           0.745               0.685
       3.4           0.728               0.670
       3.8           0.663               0.610
       4.2           0.582               0.535
       4.6           0.505               0.465
       5.0           0.467               0.430
       5.4           0.397               0.365
       5.8           0.337               0.310
       6.2           0.304               0.280
       6.6           0.255               0.235
       7.0           0.223               0.205
       7.4           0.179               0.165
       7.8           0.120               0.110
       8.2           0.033               0.030

------------------------------------------------------------
  RESULTS FOR   3.00 MeV NEUTRONS    200 ITERATIONS

       11 NEUTRON ESCAPES
        2 WITHOUT INTERACTION WITH THE DETECTOR

        8 NEUTRONS CAPTURED BEFORE        1.00 MICROSECONDS
        9 NEUTRONS NOT CAPTURED WITHIN   80.00 MICROSECONDS
      172 NEUTRONS CAPTURED IN THE COUNTING GATE

    THRESHOLD    GAMMA EFFICIENCY    TOTAL EFFICIENCY
       0.2           0.965               0.830
       0.6           0.953               0.820
       1.0           0.924               0.795
       1.4           0.895               0.770
       1.8           0.849               0.730
       2.2           0.814               0.700
       2.6           0.773               0.665
       3.0           0.750               0.645
       3.4           0.698               0.600
       3.8           0.628               0.540
       4.2           0.564               0.485
```

4.6	0.529	0.455
5.0	0.459	0.395
5.4	0.384	0.330
5.8	0.326	0.280
6.2	0.279	0.240
6.6	0.256	0.220
7.0	0.227	0.195
7.4	0.151	0.130
7.8	0.093	0.080
8.2	0.023	0.020

RESULTS FOR   5.00 MeV NEUTRONS   200 ITERATIONS

  31 NEUTRON ESCAPES
   5 WITHOUT INTERACTION WITH THE DETECTOR

   4 NEUTRONS CAPTURED BEFORE   1.00 MICROSECONDS
   2 NEUTRONS NOT CAPTURED WITHIN   80.00 MICROSECONDS
 163 NEUTRONS CAPTURED IN THE COUNTING GATE

THRESHOLD	GAMMA EFFICIENCY	TOTAL EFFICIENCY
0.2	0.957	0.780
0.6	0.951	0.775
1.0	0.939	0.765
1.4	0.902	0.735
1.8	0.883	0.720
2.2	0.877	0.715
2.6	0.822	0.670
3.0	0.785	0.640
3.4	0.730	0.595
3.8	0.669	0.545
4.2	0.589	0.480
4.6	0.521	0.425
5.0	0.460	0.375
5.4	0.436	0.355
5.8	0.380	0.310
6.2	0.325	0.265
6.6	0.288	0.235
7.0	0.233	0.190
7.4	0.160	0.130
7.8	0.117	0.095
8.2	0.049	0.040

RESULTS FOR 7.00 MeV NEUTRONS   200 ITERATIONS

  53 NEUTRON ESCAPES
  13 WITHOUT INTERACTION WITH THE DETECTOR

   4 NEUTRONS CAPTURED BEFORE   1.00 MICROSECONDS
   2 NEUTRONS NOT CAPTURED WITHIN   80.00 MICROSECONDS
 141 NEUTRONS CAPTURED IN THE COUNTING GATE

THRESHOLD	GAMMA EFFICIENCY	TOTAL EFFICIENCY
0.2	0.965	0.680

0.6	0.957	0.675
1.0	0.936	0.660
1.4	0.879	0.620
1.8	0.837	0.590
2.2	0.780	0.550
2.6	0.730	0.515
3.0	0.695	0.490
3.4	0.631	0.445
3.8	0.589	0.415
4.2	0.560	0.395
4.6	0.518	0.365
5.0	0.447	0.315
5.4	0.355	0.250
5.8	0.298	0.210
6.2	0.234	0.165
6.6	0.199	0.140
7.0	0.177	0.125
7.4	0.128	0.090
7.8	0.057	0.040
8.2	0.014	0.010
0.0	0.19000E+02	
2.0	0.16000E+02	
4.0	0.30000E+02	
6.0	0.37000E+02	
8.0	0.41000E+02	
10.0	0.42000E+02	
12.0	0.37000E+02	
14.0	0.48000E+02	
16.0	0.41000E+02	
18.0	0.36000E+02	
20.0	0.30000E+02	
22.0	0.45000E+02	
24.0	0.23000E+02	
26.0	0.23000E+02	
28.0	0.24000E+02	
30.0	0.28000E+02	
32.0	0.20000E+02	
34.0	0.12000E+02	
36.0	0.15000E+02	
38.0	0.13000E+02	
40.0	0.15000E+02	
42.0	0.90000E+01	
44.0	0.12000E+02	
46.0	0.70000E+01	
48.0	0.70000E+01	
50.0	0.13000E+02	
52.0	0.50000E+01	
54.0	0.20000E+01	
56.0	0.70000E+01	
58.0	0.40000E+01	
60.0	0.10000E+01	
62.0	0.10000E+01	
64.0	0.30000E+01	
66.0	0.40000E+01	
68.0	0.30000E+01	
70.0	0.10000E+01	

72.0	0.20000E+01
74.0	0.10000E+01
76.0	0.10000E+01
78.0	0.00000E+00
80.0	0.80000E+01
82.0	0.90000E+01
84.0	0.20000E+01
86.0	0.40000E+01
88.0	0.20000E+01
90.0	0.00000E+00
92.0	0.20000E+01
94.0	0.00000E+00
96.0	0.00000E+00
98.0	0.00000E+00
100.0	0.00000E+00
102.0	0.00000E+00
104.0	0.00000E+00
106.0	0.00000E+00
108.0	0.00000E+00
110.0	0.00000E+00
112.0	0.00000E+00
114.0	0.00000E+00
116.0	0.00000E+00
118.0	0.00000E+00
120.0	0.00000E+00
122.0	0.00000E+00
124.0	0.00000E+00
126.0	0.00000E+00
128.0	0.00000E+00
130.0	0.00000E+00
132.0	0.00000E+00
134.0	0.00000E+00
136.0	0.00000E+00
138.0	0.00000E+00
140.0	0.00000E+00
142.0	0.00000E+00
144.0	0.00000E+00

B. Comparison

(1) Capture efficiency, gamma ray detection efficiency, and total detection efficiency versus thresholds

As noted before, the total neutron detection efficiency, ϵ_{tot}, is the product of the neutron capture efficiency, ϵ_{cap}, the gamma ray detection efficiency, ϵ_γ, and the light collection efficiency, ϵ_l:

$$\epsilon_{tot} = \epsilon_{cap}\epsilon_\gamma\epsilon_l$$

We assume the light collection efficiency to be a constant 1, since the liquid scintillator has a relatively high transparency for the scintillation radiation, and the inside coating of the tank is a very good light scatterer.

After a neutron is captured by the Gd atom, gamma rays are emitted by this excited nucleus. These gamma rays then interact with the hydrocarbon based liquid scintillator, leaving in the liquid a certain amount of energy producing light. The threshold on the (minimum requirement) amount of light energy necessary for the detection of the gamma cascade is introduced by the electronics associated with the scintillator inside the neutron detector. Therefore, the gamma ray detection efficiency is depends on this threshold setting.

From plot 1-4, we can clear see that both the gamma ray detection efficiency and the total detection efficiency decrease with respect to the increase of the threshold settings.

From plot 5, we can see that these threshold settings have very little effect on the neutron capture efficiency. The reason for this is that the threshold setting controls the amount of light necessary for the detection of the gamma rays produced by the capturing nucleus, and it does not control the efficiency for capturing a neutron. As presented in a later plot, the neutron

capture efficiency does depends on the initial neutron energy.

From the noted equation, we can see that since the gamma ray detection efficiency depends on the threshold setting, even though this setting does not strongly influence the neutron capture efficiency, it does significantly influence the total neutron detection efficiency.

(2) Gamma ray detection efficiency versus initial neutron energy at different threshold setting

From plot 6 we can see that gamma ray detection efficiencies are practically constant with respect to the increase of the initial neutron energy at a threshold between 0.2 and 1.0 MeV. When the threshold is set at a relatively high values, the gamma ray detection efficiency can no longer be considered to be constant with respect to the initial neutron energy. As we can see from plot 6, the data show more fluctuations and exhibit a small decrease trend with respect to the initial neutron energy.

(3) Neutron capture efficiency versus initial neutron energy at constant threshold setting (0.2 MeV)

Plot 7 shows the well-known general trend of decreasing of the neutron capture efficiency and total neutron detection efficiency with increasing initial neutron energy. The decrease is associated with the increase in the mean free path of the neutron with increase of kinetic energy. As we mentioned before, the gamma ray detection efficiency is almost constant in this energy range because of the low threshold setting.

(4) Total neutron detection efficiency versus initial neutron energy at different threshold settings

The total neutron detection efficiency is given by the product of the gamma ray detection efficiency and the neutron capture efficiency: $\epsilon_{cap}\epsilon_{\gamma}$. Plot 8 shows

the general trend of the decrease of total neutron detection efficiency with increasing initial neutron energy at different thresholds. We can also see from this plot that the slope of the line getts smaller when the threshold is increased. The data of the total neutron detection efficiency at 7.0 MeV threshold forms a relatively flat line, compared with results obtained at 0.2 MeV threshold, which has a sharp slope.

CONCLUSION

A modified Monte Carlo simulation program has been developed to simulate the response of the 4π neutron detector. This program has been tested by comparing its predictions with the experimental results obtained by using ^{252}Cf fission source. The experimental value for the total neutron detection efficiency is 87% at 3 MeV, which is consistent with the Monte Carlo simulation result. All plots of the simulation data and the modified simulation data are agree in general with the predicted trends: the total neutron detection efficiency and the neutron capture efficiency depends on the initial energy, but the gamma ray detection efficiency is almost indenpendent on the threshold. All of these indicate that we have confidence in these simulation results.

It is thought that the this 4π neutron detector may also provide in information on the angular distributions of the neutrons. Using the labeeling techniques developed for GEOMETRY routine will allow us to explore this possibility in future studies. This goal can be achived by assigning different indicies to the wedges of the median plane.

REFERENCES

(1) R. P. Schmitt, B. K. Srivastava, I. H. Liu, et.al. "The Neutron Ball Project". Progress in Research , March,1989 , Cyclotron Institute, Texas A&M University.

(2) R. P. Schmitt, G. Nebbia, I. H. Liu, et.al. "The Neutron Ball Project". Progress in Research" , March,1988 , Cyclotron Institute, Texas A&M University.

(3) RSIC Computer Code Collection, Contributed by Nuclear Physics Department, CEA Centre d'Etudes Nucleaires de Saclay, Gif sur Yvette, France. Oak Ridge National Laboratory.

(4) J. Poitou and C. Signarbieux. "A Monte-Carlo Simulation of the Capture and Detection of Neutrons with Large Liquid Scintillator", Nuclear Instruments and Methods 1974 , 114,113 - 119.

(5) Spencer, R. R.; Gwin, R; Ingle, R. "Absolute Measurement of v p for 252 Cf Using the ORNL Large Liquid Scintillator Neutron Detector". Oak Ridge National Laboratory, ORNL/TM-7940 (internal report)

(6) Parker, J. B.; Fieldhouse, P; Mather, D. S. "Monte Carlo studies of Scintillator efficiencies and Scatter Corrections for (n, 2n) Cross Section Measurements", Nuclear Instruments and Methods 1968 , 60, 7-23.

(7) Reines, F.; Cowan, C. L.; Harrison, F. B.; Carter, D. S. "Detection of Neutrons with a Large Liquid Scintillation Counter", The Review of Scientific Instruments 1954 , 25 , 1061-1070.

(8) Jahnke, U; Ingold, G; Hilscher; Orf, H.(Hahn-Meitner-Institute Berlin); Koop, E. A.; Feige, G; Brandt, R. (Philipps-Universitat), "A 4 p Neutron Multiplicity Detector for Heavy-Ion Experiment", Lecture Notes in Physics 1982 , 178 , 179-201.

(9) Diven, B. C.; Martin, H. C.; Taschek, R. F.; Terrell, J. "Multiplicities of Fission Neutrons", Physical Review 1956 , 101 , 1012-1015.

(10) Hicks, D. A; Ise. J; Pyle, R. "Probabilities of Prompt-Neuton Emission from Spontaneous Fission", Physical Review 1956, 101 , 1016-1020.

LIQUID SCINTILLATOR TANK
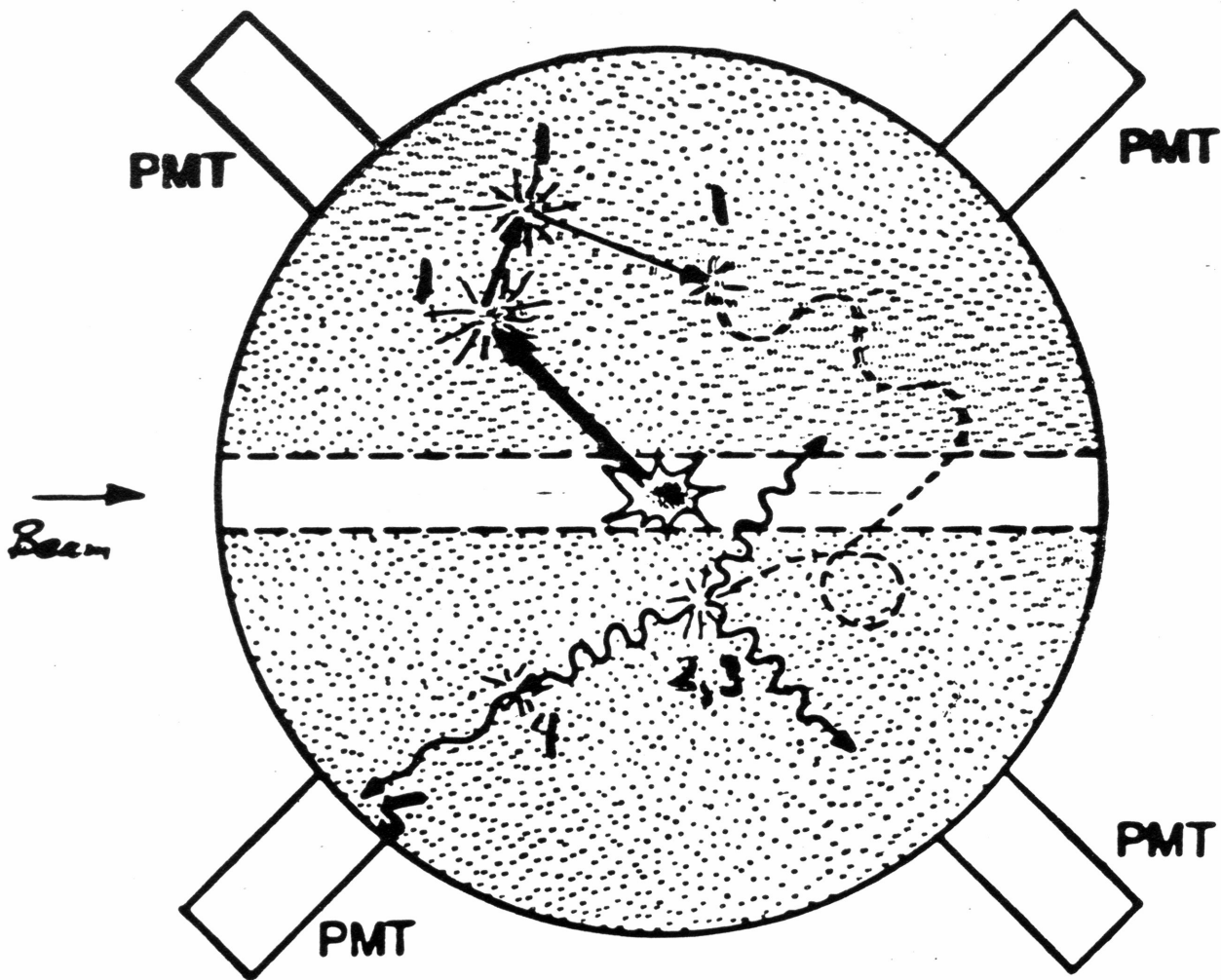
FIG. 1

1. Slow 'em down
2. Capture with Gd
3. Produce γ's
4. Convert to light
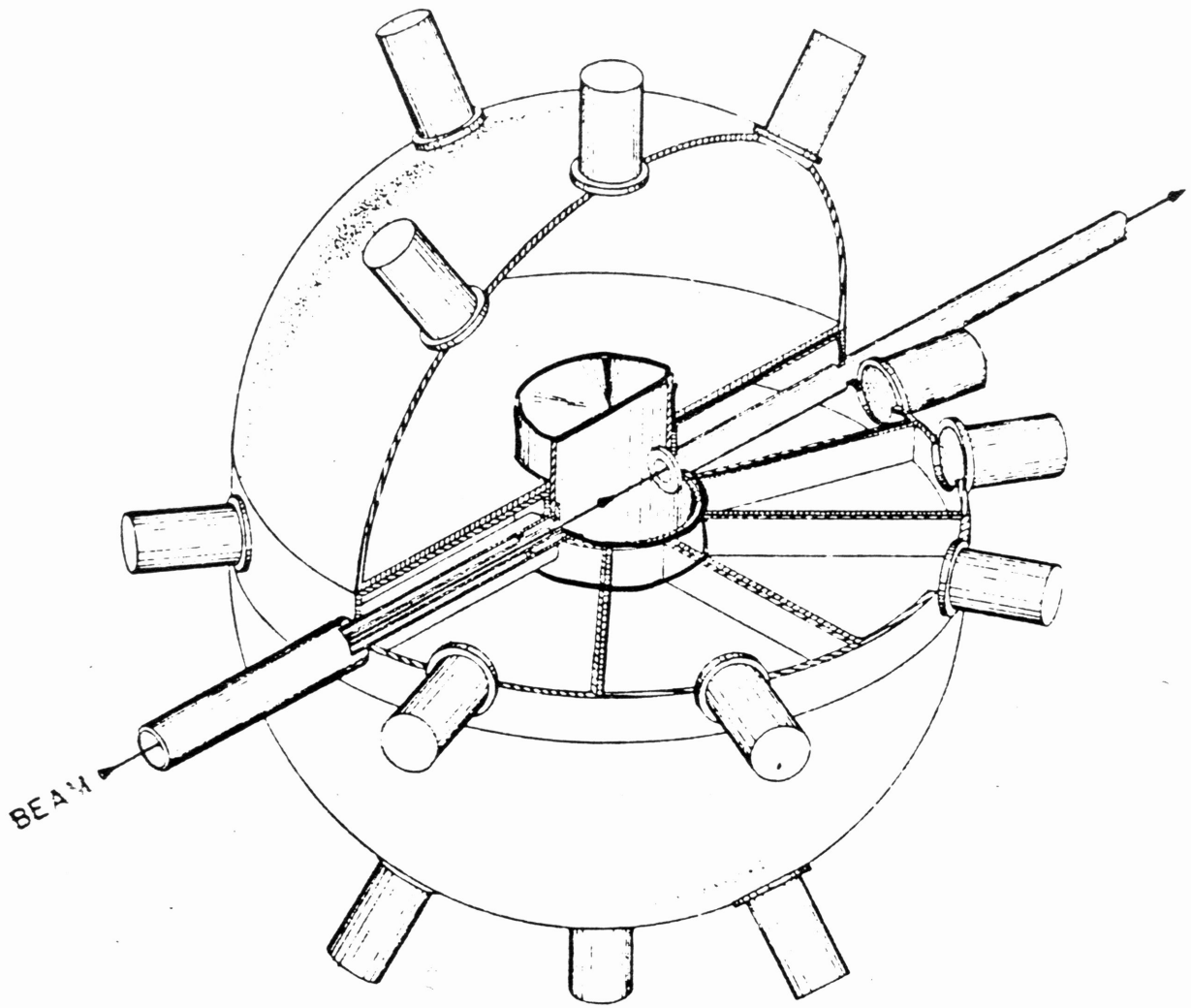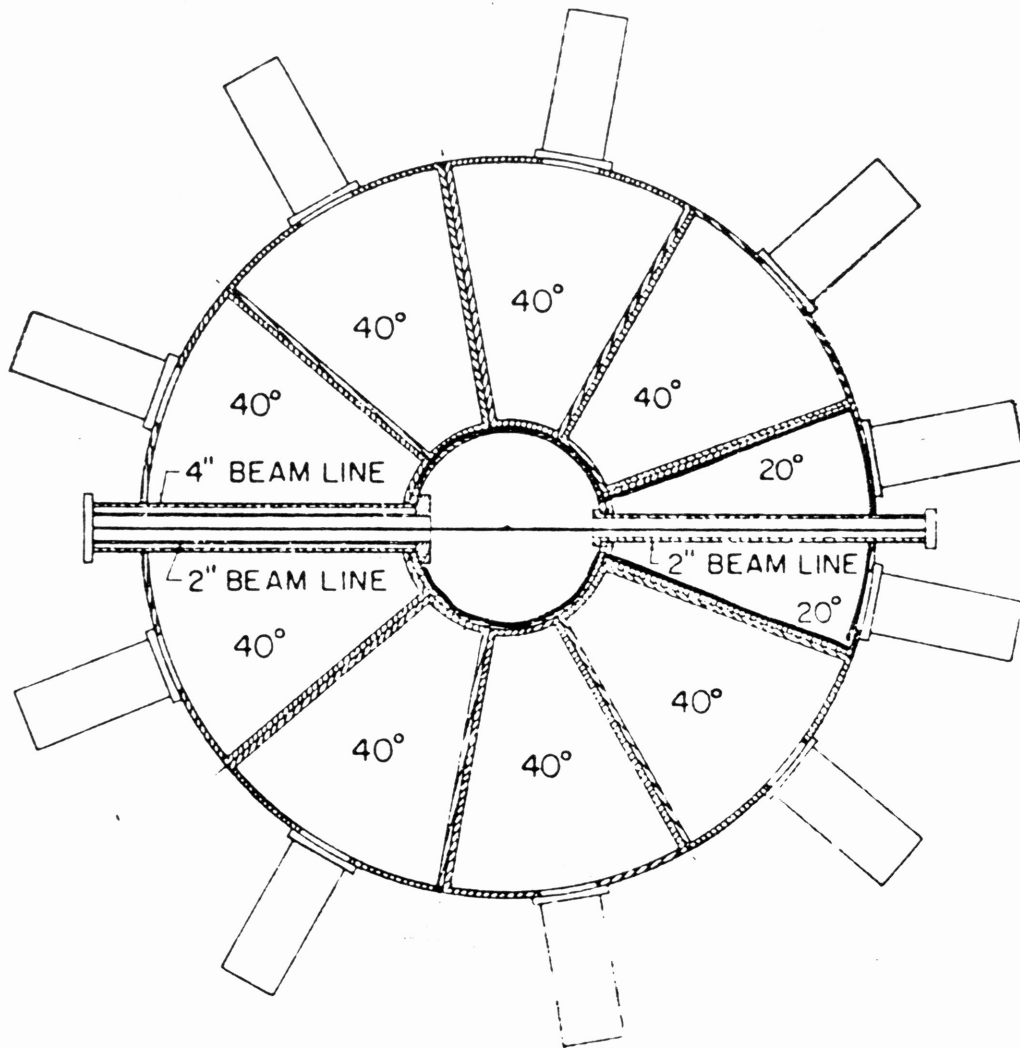5. Detect light with phototubes
6. Count blip's

BEAM

FIG. 2

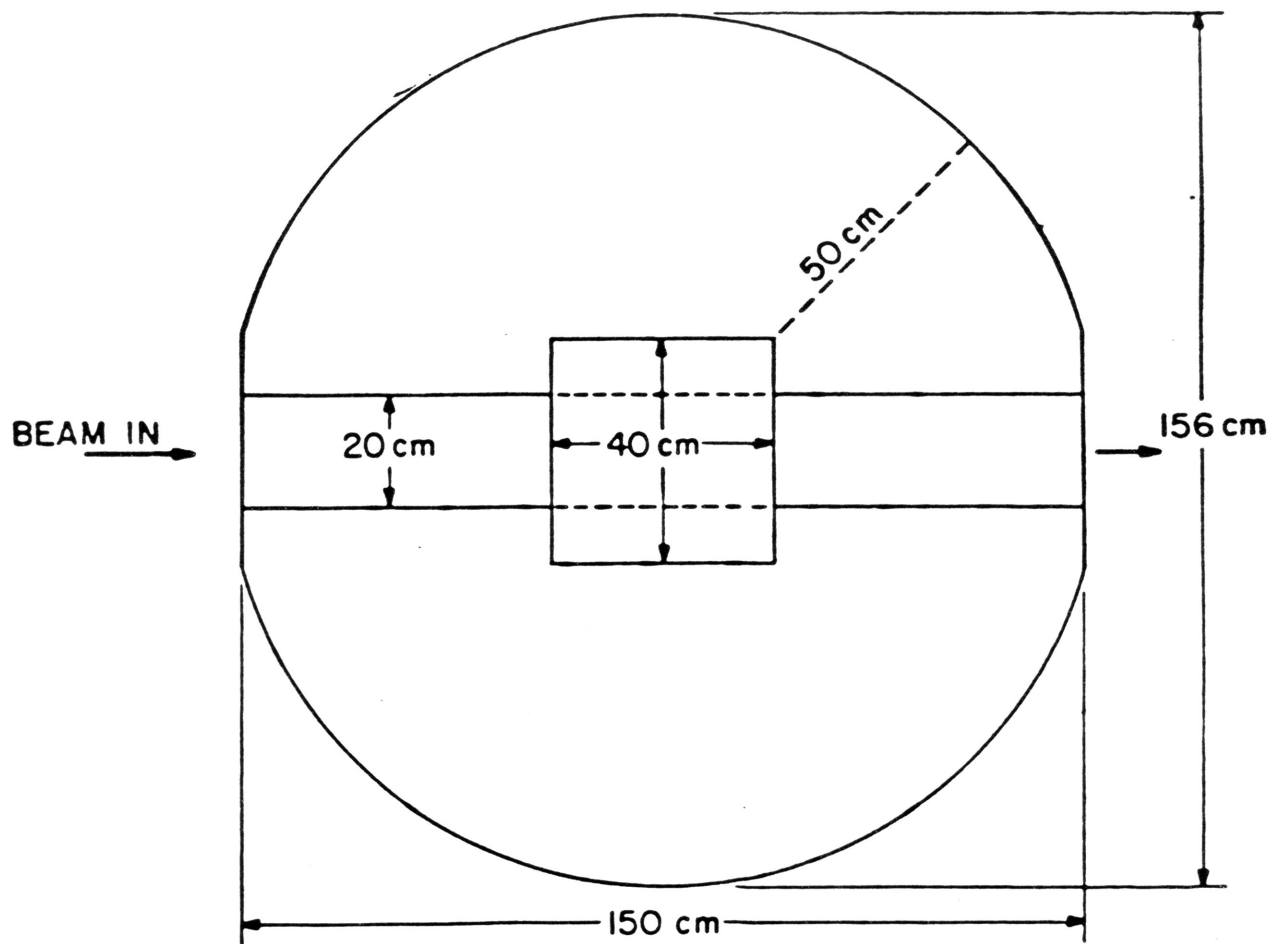FIG. 3: MEDIAN PLANE

BEAM IN →

20 cm

40 cm

50 cm

156 cm

150 cm

FIG. 4

Monte Carlo Program
written by: J. Poitou
C. Signarbieux. (1973)

LOC — Initializations Input of cross sections

MAIN

RALENT — slowing down and capture of the neutrons

GEOM. — Trajectory between two ...

EMIGAM — capture gamma cascades emission

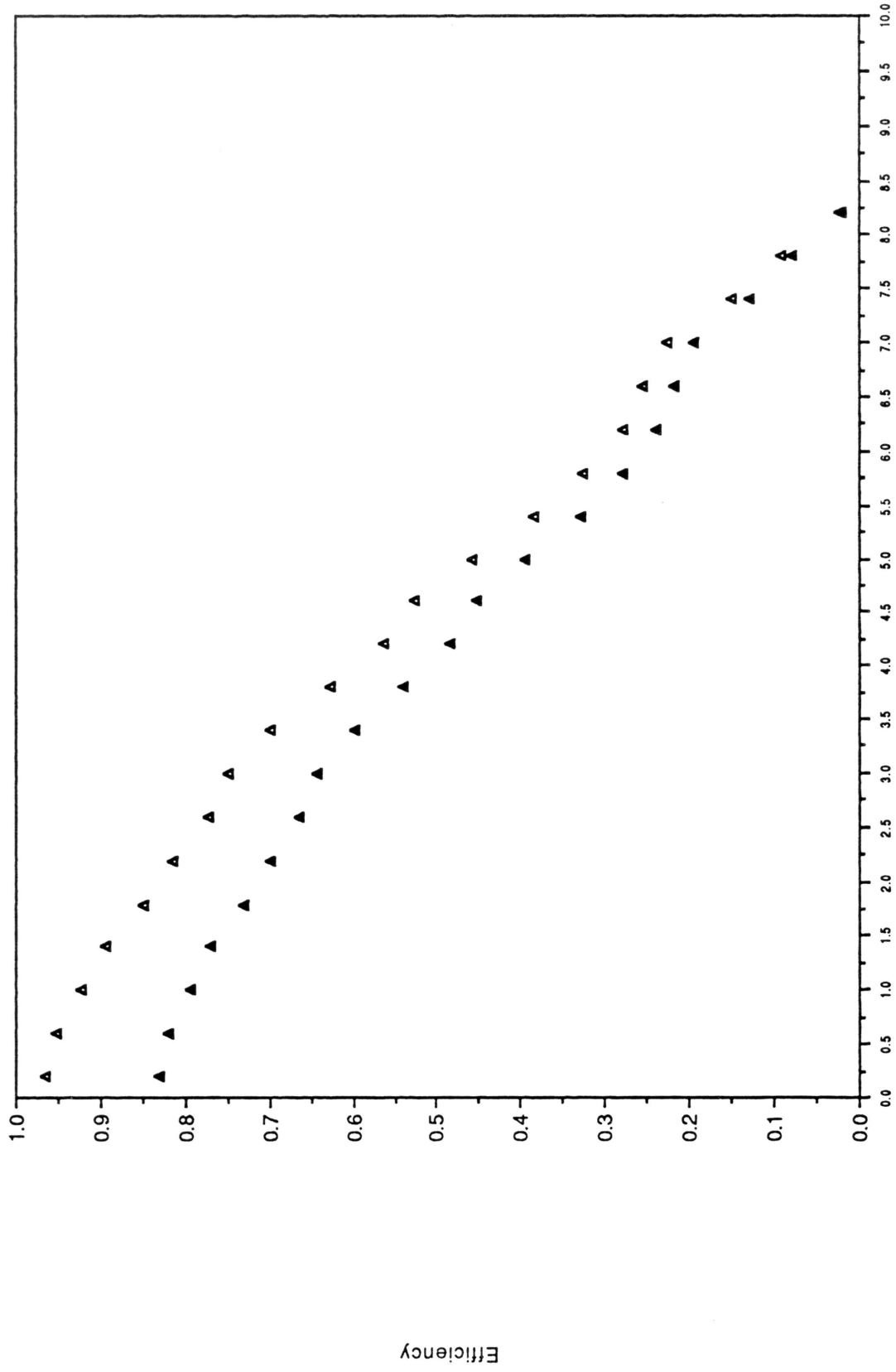**SLOWIN** — Compton scattering of the gammas
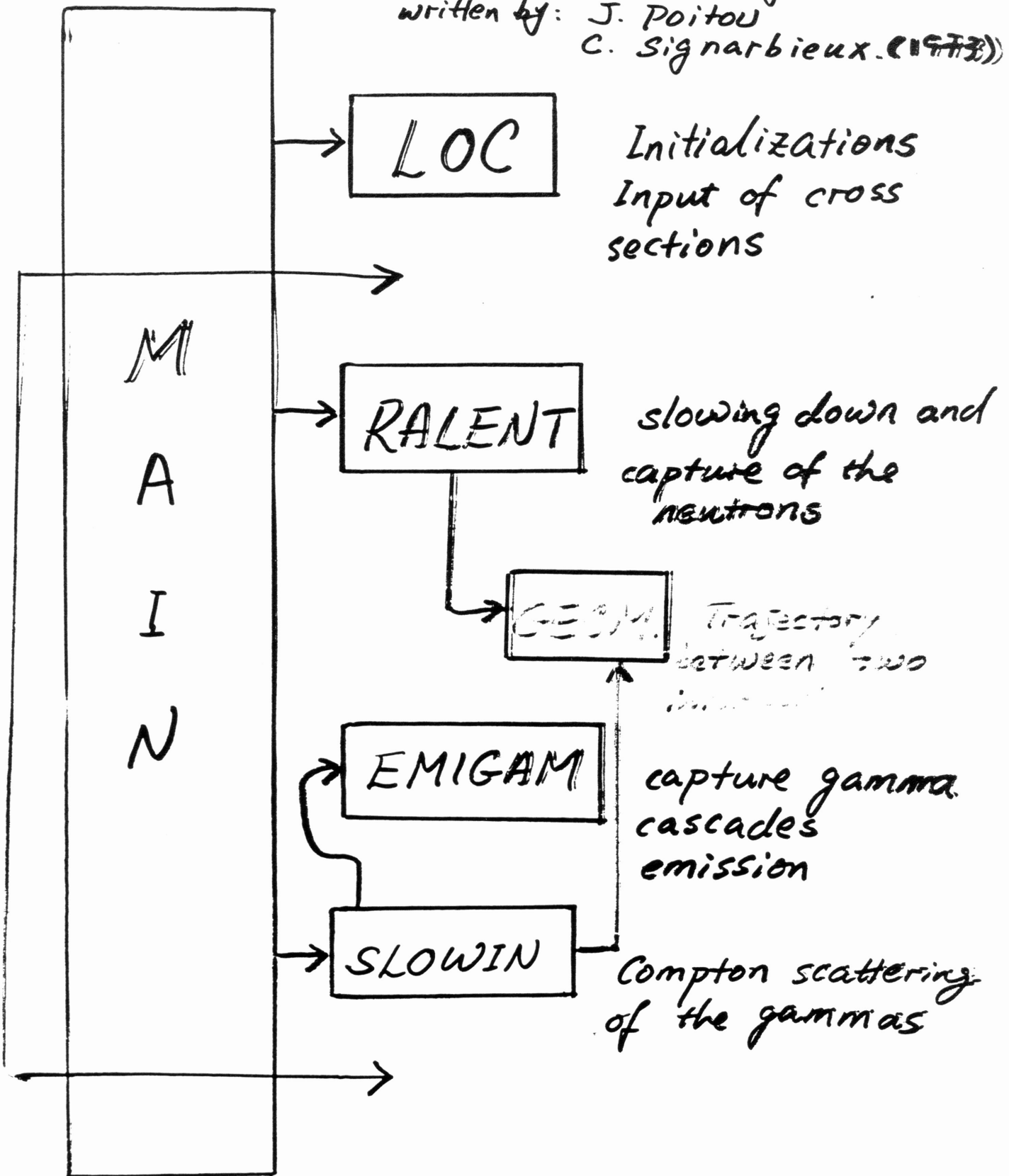
FIG. 5

Results for 1.00 MeV neutrons
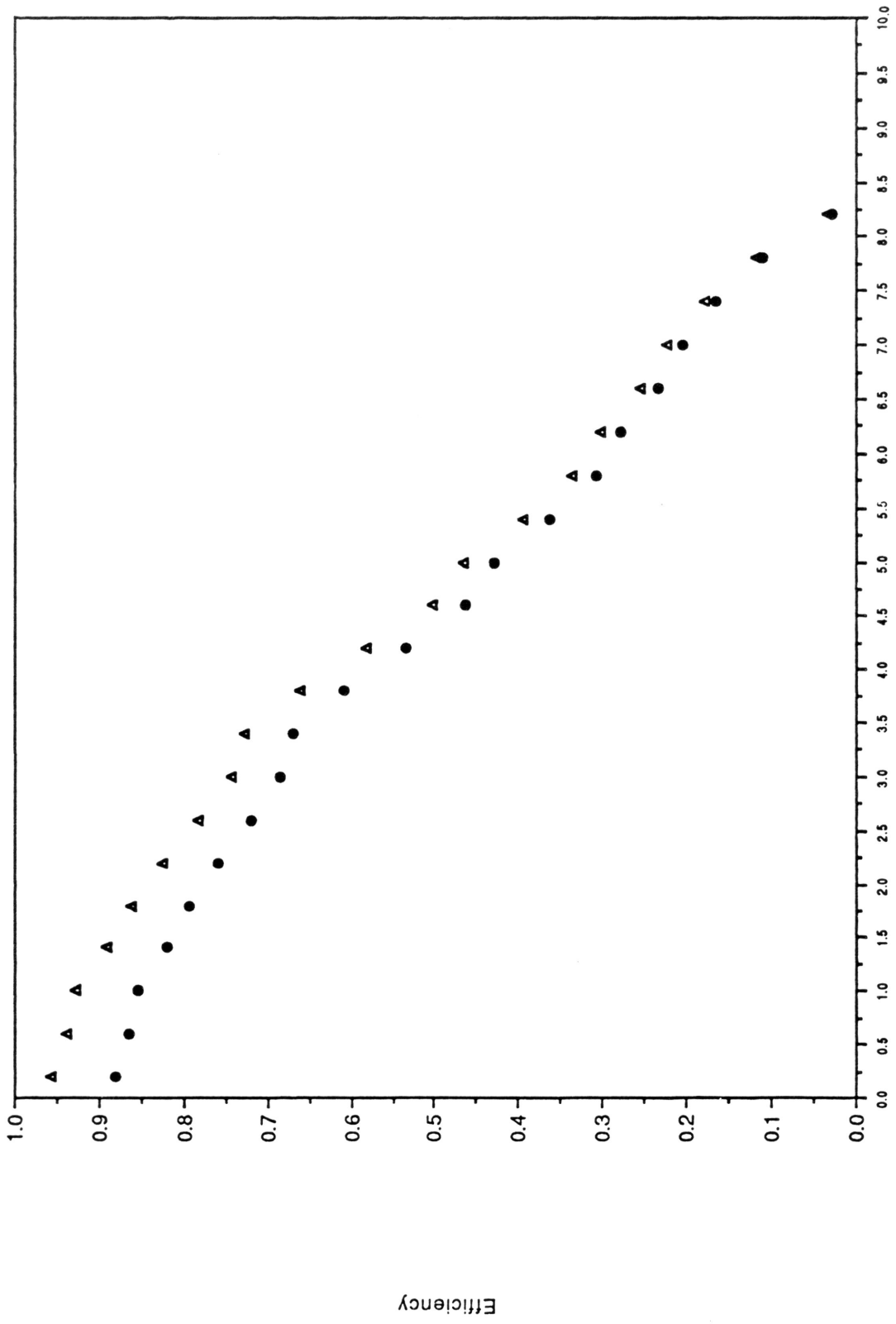
Efficiency

Threshold

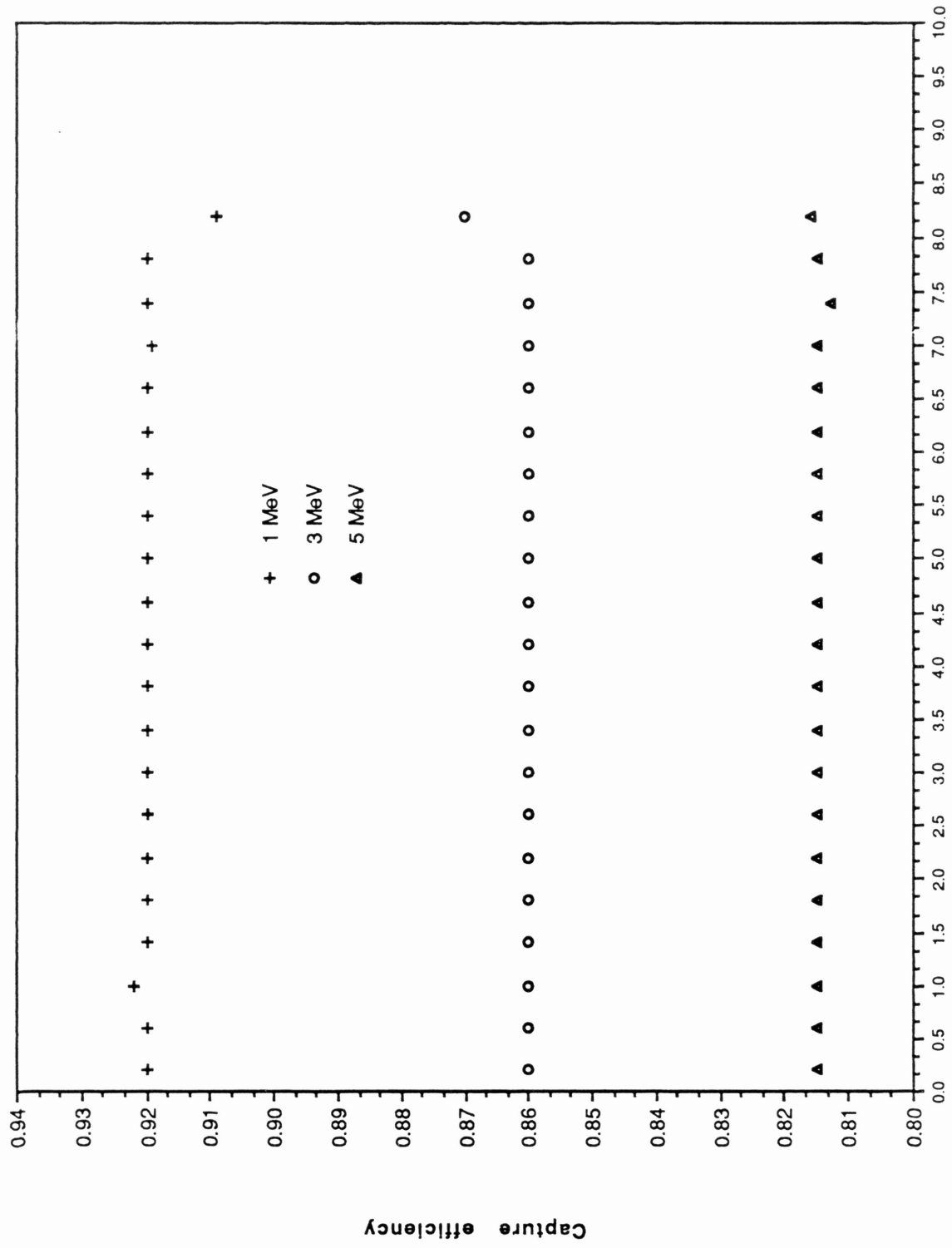PLOT 1

Results for 3.00 Mev Neutrons

Efficiency

Threshold

PLOT 2

Results for 5.00 MeV Neutrons

Efficiency vs. Threshold

PLOT 3

Results for 7.00 MeV Neutrons

Total Efficiency

Threshold

PLOT 4
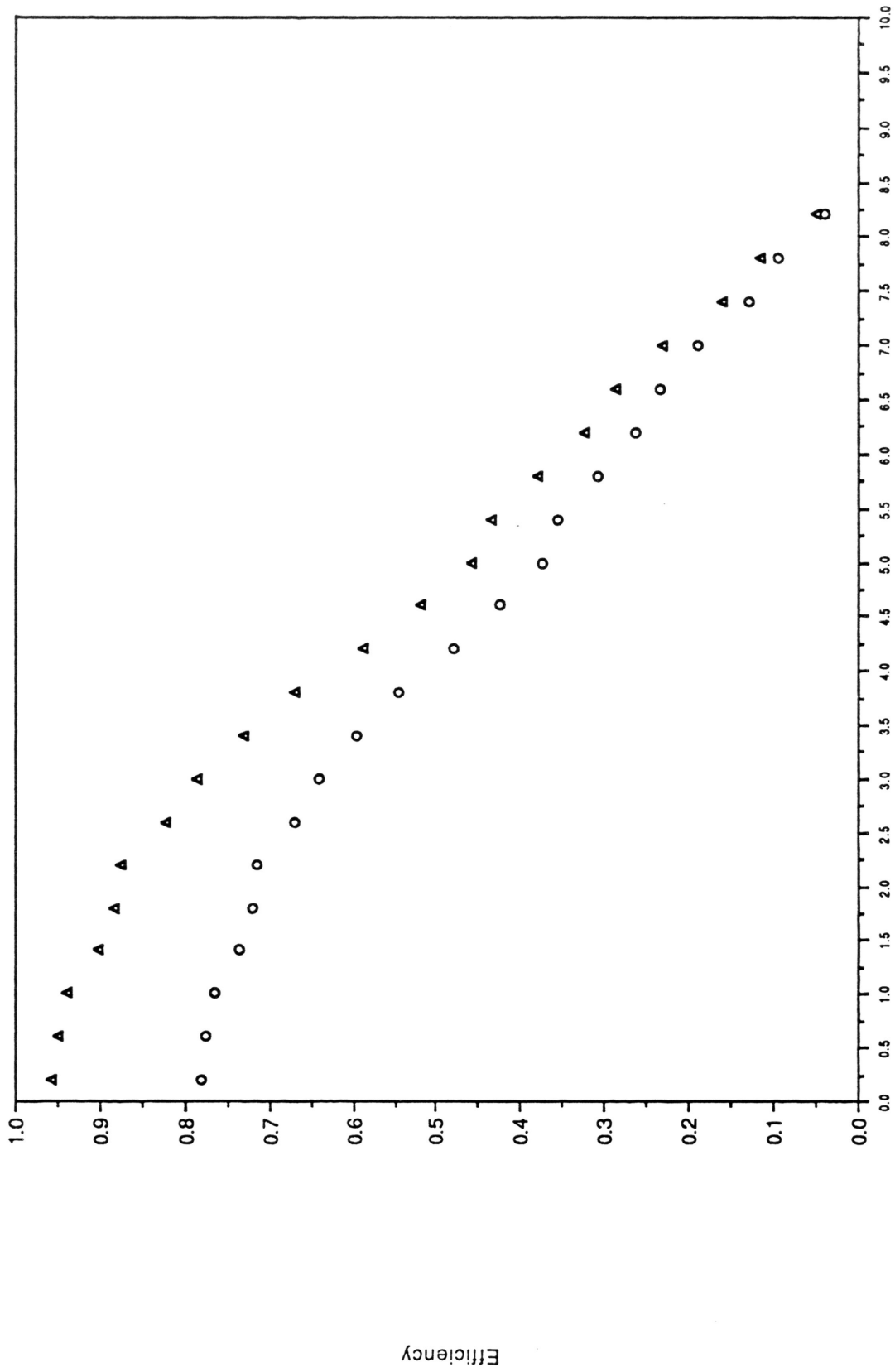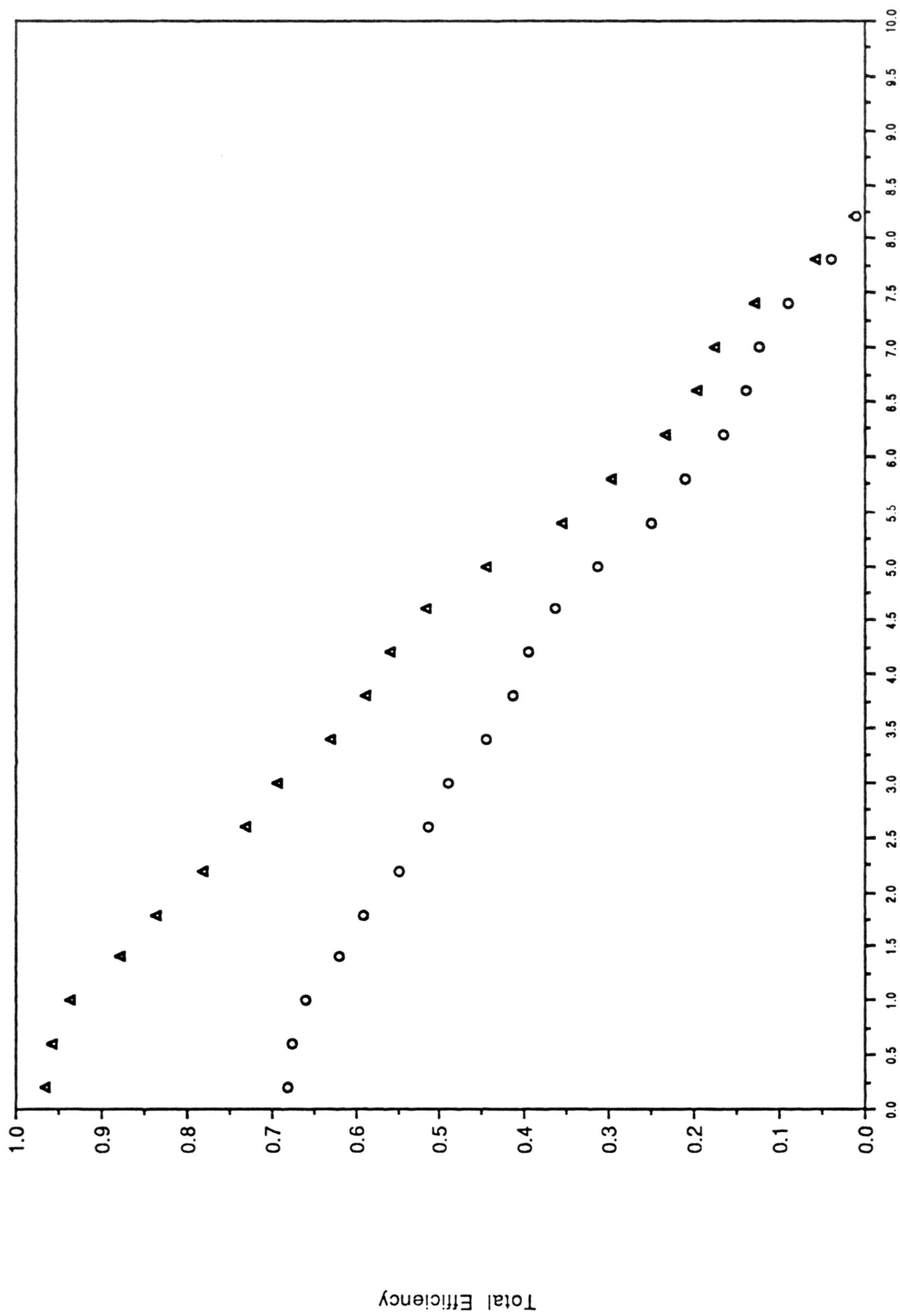
Capture efficiency vs. Threshold
at different energy

1 MeV +
3 MeV o
5 MeV ◀

Capture efficiency

Threshold

PLOT 5

44no3.realdat

	Threshold	1 MeV	3 MeV	5 MeV
1	0.200	0.920	0.860	0.815
2	0.600	0.920	0.860	0.815
3	1.000	0.922	0.860	0.815
4	1.400	0.920	0.860	0.815
5	1.800	0.920	0.860	0.815
6	2.200	0.920	0.860	0.815
7	2.600	0.920	0.860	0.815
8	3.000	0.920	0.860	0.815
9	3.400	0.920	0.860	0.815
10	3.800	0.920	0.860	0.815
11	4.200	0.920	0.860	0.815
12	4.600	0.920	0.860	0.815
13	5.000	0.920	0.860	0.815
14	5.400	0.920	0.860	0.815
15	5.800	0.920	0.860	0.815
16	6.200	0.920	0.860	0.815
17	6.600	0.920	0.860	0.815
18	7.000	0.919	0.860	0.815
19	7.400	0.920	0.860	0.813
20	7.800	0.920	0.860	0.815
21	8.200	0.909	0.870	0.816

DATA FOR PLOT 5

Gamma Efficiency vs. Neutron Energy
at different thresholds
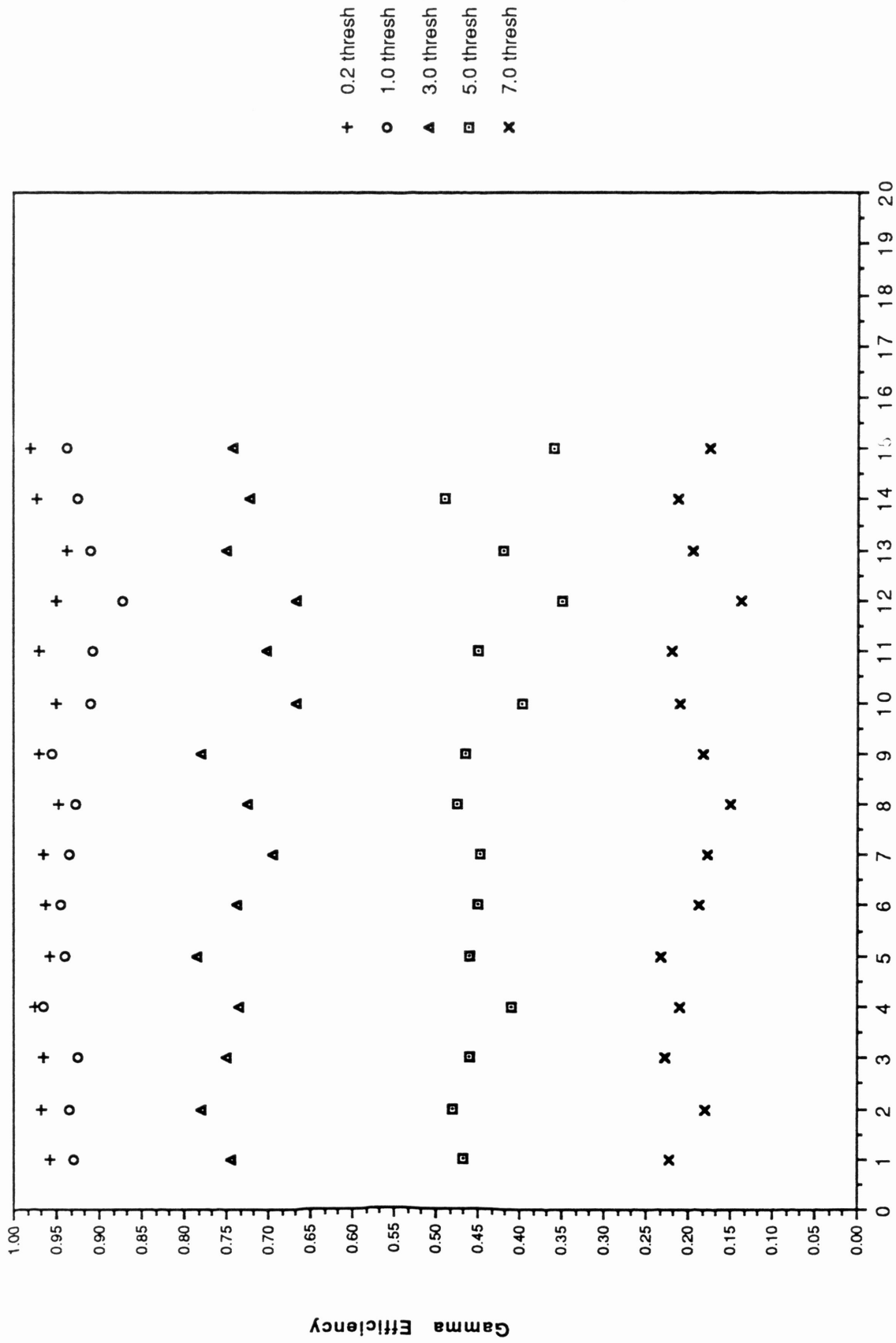
Gamma Efficiency

Neutron E

PLOT 6 (without fit)

+ 0.2 thresh
o 1.0 thresh
▲ 3.0 thresh
▫ 5.0 thresh
✕ 7.0 thresh

Gamma Efficiency vs. Neutron Energy
at different thresholds

Gamma Efficiency

Neutron E (MeV)

PLOT 6 (with fit)

0.2 thresh   +
1.0 thresh   o
3.0 thresh   ▲
5.0 thresh   ✕
7.0 thresh   □

44no2dat

DATA FOR PLOT 6
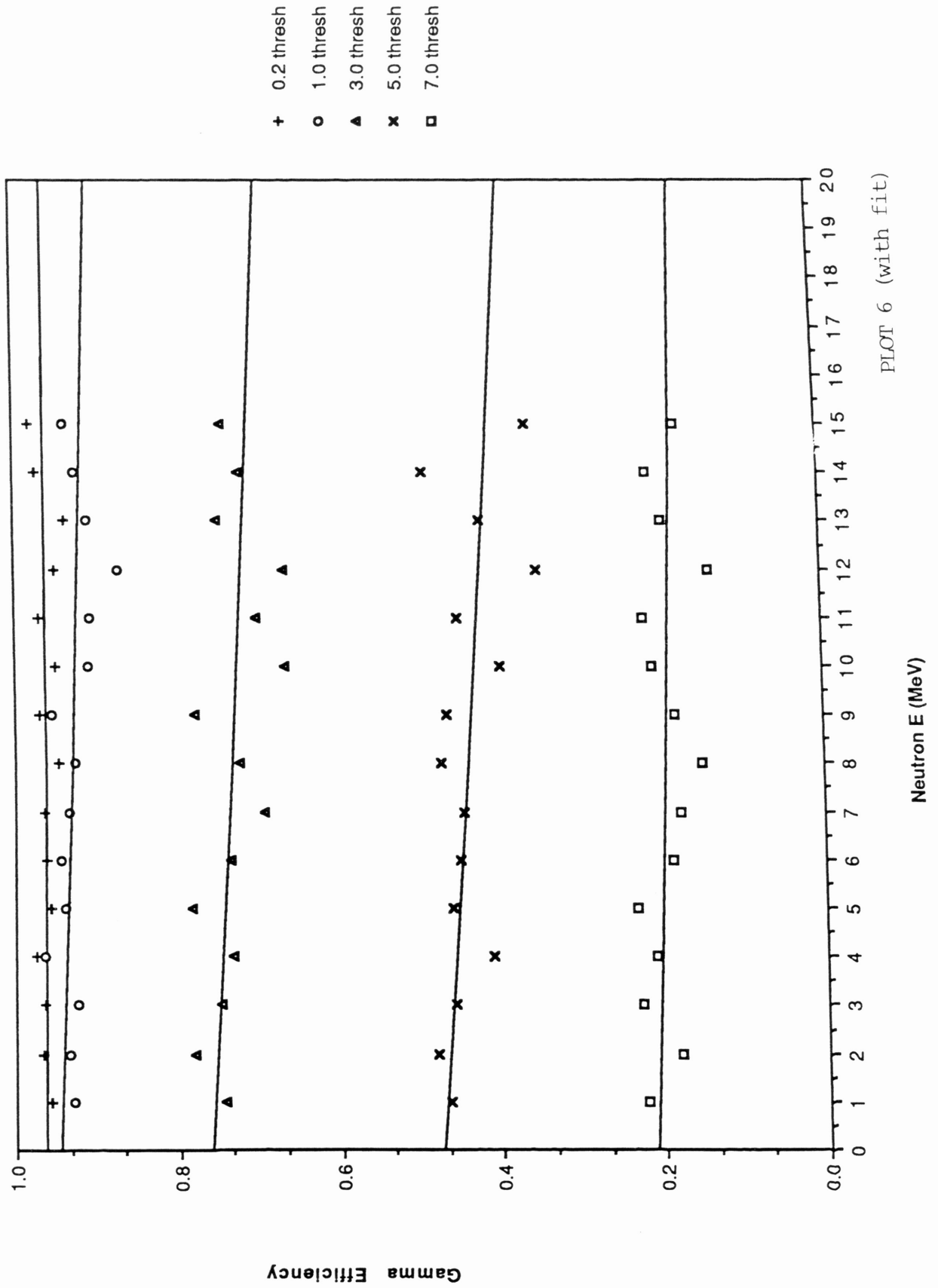
Neutron E	0.2 thresh	1.0 thresh	3.0 thresh	5.0 thresh	7.0 thresh
1 1.000	0.957	0.929	0.745	0.467	0.223
2 2.000	0.967	0.934	0.781	0.481	0.180
3 3.000	0.965	0.924	0.750	0.459	0.227
4 4.000	0.976	0.964	0.735	0.410	0.211
5 5.000	0.957	0.939	0.785	0.460	0.233
6 6.000	0.963	0.944	0.738	0.450	0.188
7 7.000	0.965	0.936	0.695	0.447	0.177
8 8.000	0.947	0.928	0.724	0.474	0.151
9 9.000	0.969	0.954	0.779	0.466	0.183
10 10.000	0.951	0.911	0.667	0.398	0.211
11 11.000	0.969	0.908	0.702	0.450	0.221
12 12.000	0.949	0.872	0.667	0.350	0.137
13 13.000	0.938	0.911	0.750	0.420	0.196
14 14.000	0.972	0.926	0.722	0.491	0.213
15 15.000	0.979	0.938	0.742	0.361	0.175

Monte Carlo Simulation Results
0.2 threshold

Gamma Eff. ▲
Cap. Eff. +
Total Eff. o

Efficiency

Neutron E

PLOT 7

43new

DATA FOR PLOT 7
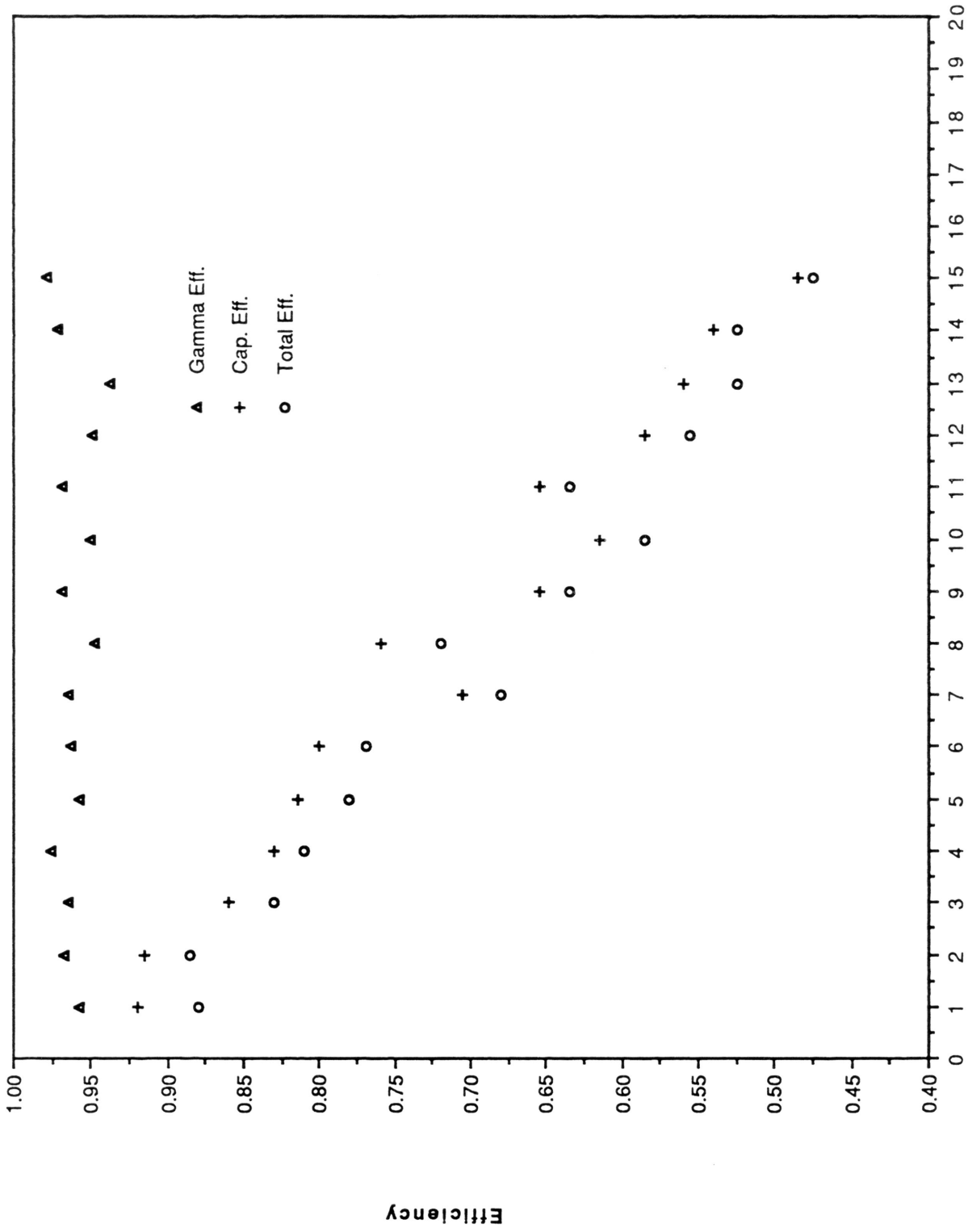
	Gamma Eff.	Cap. Eff.	Total Eff.	Neutron E
1	0.957	0.920	0.880	1.000
2	0.967	0.915	0.885	2.000
3	0.965	0.860	0.830	3.000
4	0.976	0.830	0.810	4.000
5	0.957	0.815	0.780	5.000
6	0.963	0.800	0.770	6.000
7	0.965	0.705	0.680	7.000
8	0.947	0.760	0.720	8.000
9	0.969	0.655	0.635	9.000
10	0.951	0.615	0.585	10.000
11	0.969	0.655	0.635	11.000
12	0.949	0.585	0.555	12.000
13	0.938	0.560	0.525	13.000
14	0.972	0.540	0.525	14.000
15	0.979	0.485	0.475	15.000

Total Efficiency vs. neutron E
at different threshold

Efficiency

Neutron E

PLT 8 (with fit)

Total Efficiency vs. neutron E
at different threshold
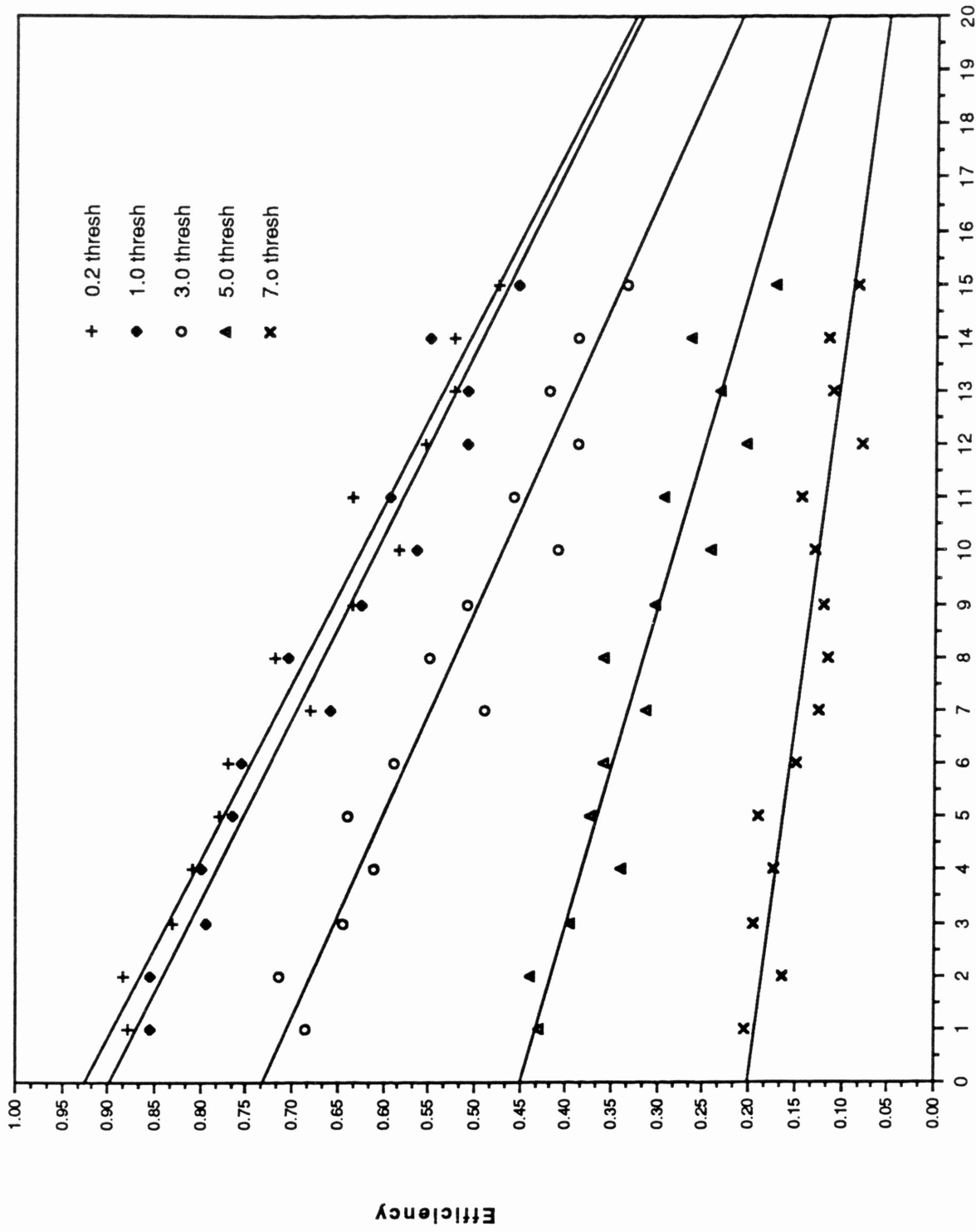
Efficiency

Neutron E

0.2 thresh   +
1.0 thresh   ●
3.0 thresh   ○
5.0 thresh   ▲
7.0 thresh   ✕
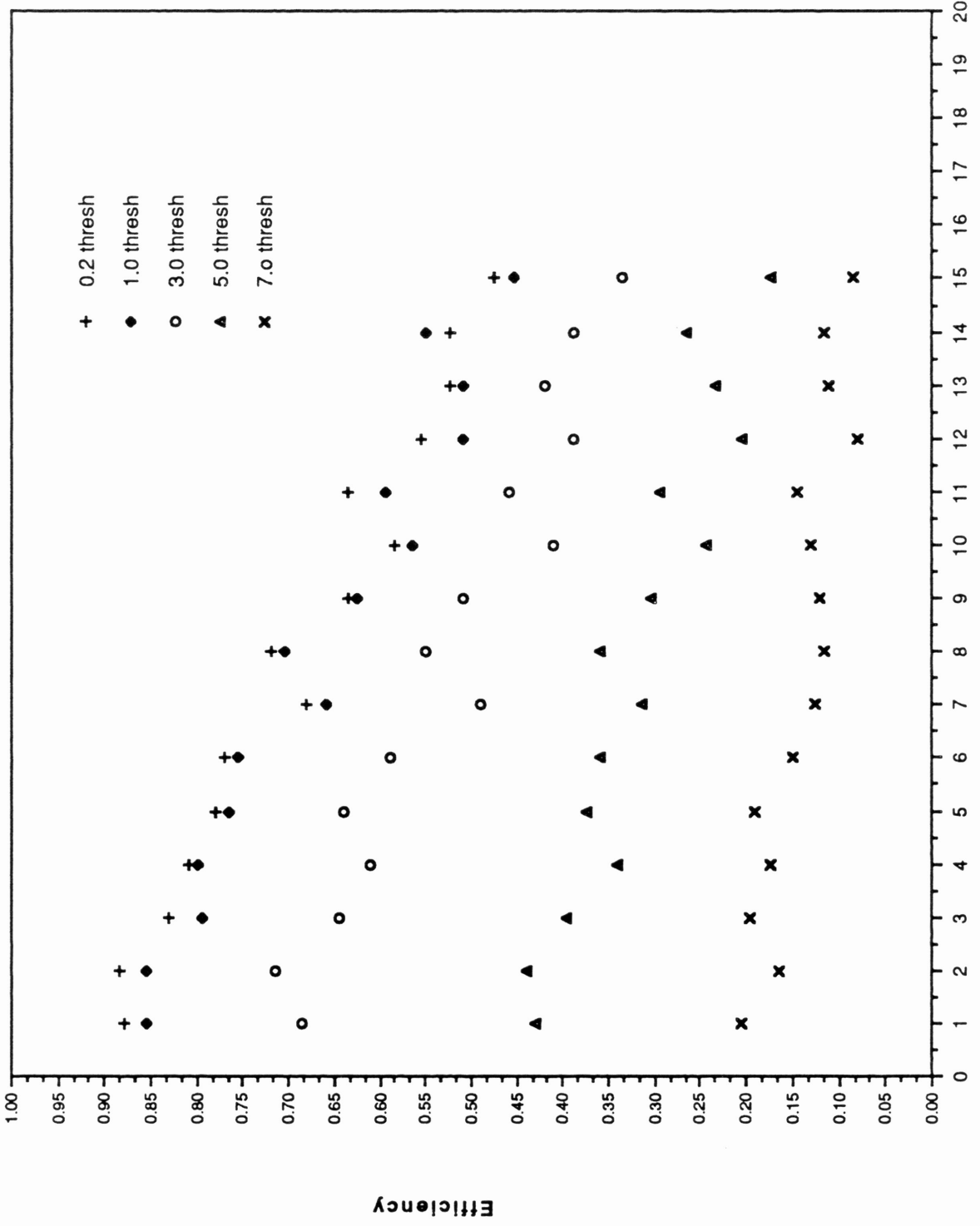
PLOT 8 (without fit)

44dat

	0.2 thresh	Neutron E	1.0 thresh	3.0 thresh	5.0 thresh	7.o thresh
1	0.880	1.000	0.855	0.685	0.430	0.205
2	0.885	2.000	0.855	0.715	0.440	0.165
3	0.830	3.000	0.795	0.645	0.395	0.195
4	0.810	4.000	0.800	0.610	0.340	0.175
5	0.780	5.000	0.765	0.640	0.375	0.190
6	0.770	6.000	0.755	0.590	0.360	0.150
7	0.680	7.000	0.660	0.490	0.315	0.125
8	0.720	8.000	0.705	0.550	0.360	0.115
9	0.635	9.000	0.625	0.510	0.305	0.120
10	0.585	10.000	0.565	0.410	0.245	0.130
11	0.635	11.000	0.595	0.460	0.295	0.145
12	0.555	12.000	0.510	0.390	0.205	0.080
13	0.525	13.000	0.510	0.420	0.235	0.110
14	0.525	14.000	0.550	0.390	0.265	0.115
15	0.475	15.000	0.455	0.335	0.175	0.085

DATA FOR PLOT 8